Tutor/s

Dr. Paul Lloyd-Williams
Departament de Química Inorgànica i Orgànica, Secció de Química Orgànica

Grau de Química

Treball Final de Grau

Comparison of the synthesis of *meta*- and *para*-substituted heterocyclic ligands for complexation with metals. Study of the resulting complexes by X-ray crystallography
Comparació de la síntesi de lligands heterocíclics substituïts en *meta* i *para* per a la complexació de metalls. Estudi dels compostos resultants per cristal·lografia de raigs-X

Neus Santiago i Domínguez

June 2021

UNIVERSITAT DE BARCELONA

B:KC Barcelona Knowledge Campus
Campus d'Excel·lència Internacional

Aquesta obra esta subjecta a la llicència de:
Reconeixement–NoComercial-SenseObraDerivada

http://creativecommons.org/licenses/by-nc-nd/3.0/es/

"Hope" is the thing with feathers
That perches in the soul,
And sings the tune without the words.
And never stops at all.

Emily Dickinson

M'agradaria agrair primerament al Dr. Paul Lloyd-Williams per guiar-me durant tot aquest procés, pels consells i per animar-me a no perdre l'optimisme en cap moment. També, m'agradaria agrair al Dr. Jordi Garcia, perquè conjuntament amb en Paul, ha estat disponible en qualsevol moment per donar consell o ajut.

D'altra banda, agrair a totes les persones del lab 63/64, especialment al Javier González i la Emma Peregrín, que han estat cada dia suportant les meves preguntes i sempre m'han brindat ajut amb un somriure.

Per acabar, però no menys importants, a la meva família i amics per aportar-me energia en els dies que més necessitava i el suport necessari, no només durant el temps del TFG sinó durant tota la carrera.

A tots moltes gràcies.

REPORT

CONTENTS

1. SUMMARY

Organic compounds with conjugated azo groups (-N=N-) allow reversible isomerization between the *cis* and *trans* isomers under UV irradiation. As a consequence of this isomerization, there are changes in the physicochemical properties of the compounds such as their refractive indices, dielectric constants, redox potentials and their geometric structures.

This characteristic makes such azo compounds interesting in fields of study such as the development of liquid crystals, photo switches,(1) or even as therapeutic agents and drug delivery systems.(2)

Our research group is interested in the synthesis of new ligands incorporating azo and imine groups capable of coordinating with metal cations (especially with lanthanides) in order to obtain new nanomaterials that have the properties of single-molecule magnets (SMM) in which irradiation with UV light can modulate their properties.

This report is a continuation of previous work carried out in our group and addresses the synthesis of a *meta*-substituted ligand that provides an interesting structure for coordination with metal cations. The synthesis of analogous *para*-substituted ligands was also carried out for comparison purposes (**Fig 1**).

Furthermore, studies of the crystal structure of both the free-ligands and those coordinated with metal cations were carried out by X-ray crystallography.

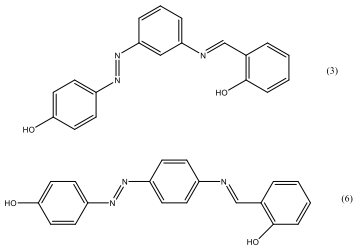

Fig. 1 Ligands synthesized in this work

Keywords: Azo groups, photo switches, single-molecule magnets, liquid crystals, ligands

2. RESUM

Els compostos orgànics amb grups azo conjugats (-N=N-) permeten isomeritzacions reversibles entre els isòmers *cis* i *trans* sota la irradiació de llum UV. Aquestes isomeritzacions provoquen canvis en les seves propietats fisicoquímiques com pot ser els índex de refracció, les constants dielèctriques, els potencials redox o la seves estructures geomètriques.

Aquesta peculiaritat és el que fa que siguin tan importants en camps d'estudi de cristalls líquids, fotointerruptors,(1) o inclús agents terapèutics o com a administradors de fàrmacs.(2)

El grup d'investigació en el qual ens trobem està interessat en la síntesi de nous lligands que incorporen grups azo i imina capaços de coordinar-se amb cations metàl·lics (especialment amb lantànids) per obtenir nous nanomaterials amb propietats que els fessin imants monomoleculars (SMM) on el seu comportament es pot veure modificat per la irradiació de llum.

Aquest treball és una continuació de treballs anteriors realitzats en el mateix grup amb la incorporació dels lligands en *meta* que aporten interès estructural en la coordinació. La síntesis dels lligands *para* substituïts també s'ha portat en pràctica amb fins comparatius (**Fig 2**).

A més a més, s'han fet estudis de la estructura cristal·lina del lligand lliure i el lligand coordinat amb cations metàl·lics per cristal·lografia de raigs-X.

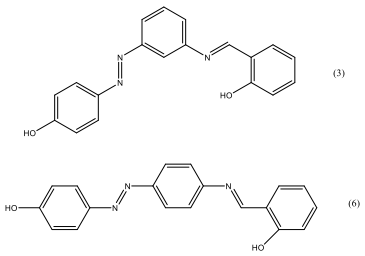

Fig. 2 Lligands sintetitzats en aquest treball

Paraules clau: Grups azo, fotointerruptors, imants mononuclears, cristalls líquids, lligands

3. INTRODUCTION

As our requirements for information storage increases exponentially, the necessity of storing increasingly large amounts in devices of ever smaller physical size is becoming more and more important.

Azo compounds and their coordination complexes may find application in the development of technological resources such as SMMs and also in certain drug delivery systems. The potential use of SMMs in ultra-high density information storage and ultra-fast information processing is currently an area that is being intensively studied.(3)

3.1 SMMs

Single molecule magnets (SMMs) consist of an inner magnetic core surrounded by organic ligands. To intensify the magnetic interactions between the core ions and the ligands and to increase their conducting properties, SMMs usually have delocalized bonds. The properties of SMMs can be modulated by changing the metals ions that maintain the overall structure or by changing the organic ligands themselves. Consequently, a large variety of sizes and structures are possible. Such complexes often give high quality crystals which makes their study by X-ray crystallography easy.

With respect to their physical properties, SMMs combine characteristics of a classical magnet with nanoscale characteristics, such as quantum coherence, which may be important in the physics of storage devices.(4,5)

At low temperatures (under 2K), SMMs molecules present a hysteresis loop and a single characteristic slow relaxation time that obeys the Arrhenius law, $k = A \times e^{-\left(\frac{E_a}{RT}\right)}$. The slow relaxation of magnetization occurs due to the quantum tunnelling of magnetization (QTM), which has been studied since the 1980s, and produces the characteristic steps at the resonance fields in the hysteresis curve.(4,6)

The hysteresis loop is the representation of how the magnetization changes depending on the magnetic field. It increases with the magnetic field until magnetization saturation. If, on the

other hand, the magnetic field starts decreases, the magnetization also decreases, but by a different path. This irreversible property is what is known as hysteresis. The width of the hysteresis loop shown in **Fig. 3** depends not only on the temperature at which the measurement is carried out, but also on the magnetic field.

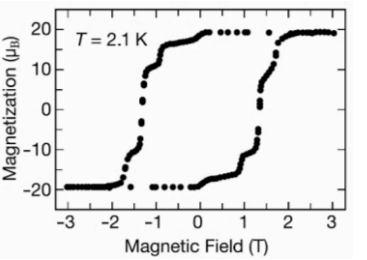

Fig. 3 Example of hysteresis loop

In 1993, the first SMM complex, $[Mn_{12}O_{12}(O_2CCH_3)_{16}(H_2O)_4]\cdot 4H_2O\cdot 2CH_3CO_2H$ was synthesized by Sessoli, Gatteschi, Caneschi and Novak[7] and it's three-dimensional X-ray structure is shown below.

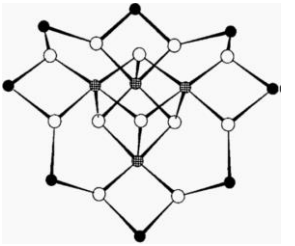

Fig. 4 $[Mn_{12}O_{12}(O_2CCH_3)_{16}(H_2O)_4]\cdot 4H_2O\cdot 2CH_3CO_2H$

The complex presents a cubic structure in the centre with μ_3-O^{2-} bridges shown in white and Mn^{IV} ions shown in grey. The oxygen bridges contribute to forming the core and interacting with the Mn^{III} ions that envelope the cube.[8]

The first SMMs were synthesized with transition metals such as Mn^{III}, Co^{II} or Ni^{II}, but recent studies show that lanthanides could improve the properties of SMMs. Lanthanide ions used in such studies include terbium (III), dysprosium (III), erbium (III) and holmium (III).[9]

On account of the increasing number of studies in the field of new SMM synthesis, advances are continually being made. For example, in 2018, the first SMM with a blocking temperature above 77 K was synthesized by Layfield.(10)

3.2 AZO COMPOUNDS AND THEIR PROPERTIES

Azobenzene derivatives have become one of the most well-known light-controlled molecular switches.(11) Since the discovery of the *cis/trans* isomerization about their azo-double bond under UV irradiation and their easy chemical preparation, they have been integrated into a variety of functional systems.

Normally, *cis/trans* isomerization can be brought about by thermal or photochemical means. The *trans* form is normally more stable but irradiation with UV light brings about its isomerization to the *cis* form. Isomerization can also occur thermally, with the *cis* form often being unstable at rt, although exceptions to this have been reported recently.(12)

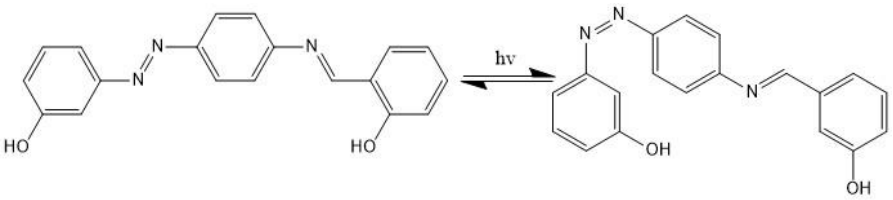

Fig. 5 *cis/trans* Isomerization

cis/trans Isomerization in azo derivatives can be useful in molecular switches as well as in certain drug delivery systems. For example, this property is used in near infrared (NIR) light-triggered anticancer drugs. Azobenzene's are incorporated in the mesopores of the silica and the continuous isomerization under UV and visible light acts as a molecular impeller.(13)

This report will focus on the comparison between *meta* and *para*-substituted ligands for the synthesis of potential SMM complexes.

4. OBJECTIVES

The aim of this project is to synthesize certain *meta* and *para*-substituted heterocyclic ligands and to compare the experimental procedures for their obtention together with their complexation properties with metal ions.

Both the free ligand and the metal-complexed structures will be studied by X-ray crystallography.

5 BACKGROUND TO THE SYNTHETIC CHEMISTRY

The work described in this report forms part of a continuing collaborative project between Dr. Carolina Sañudo of the GMMF group (Inorganic Chemistry Section) and Dr. Jordi García of the SMBioCom group (Organic Chemistry Section) at the Facultat de Química, Universitat de Barcelona.

In earlier work carried out by Amin Boulahfa[14] and Javier González,[15] effective synthetic route to ligand **6** (also known as AZO**1**) was developed and preliminary work on its complexation with metal ions was also attempted.

In parallel with the work described in this report, Diego Abad[16] has been able to improve the crystallization procedures for the metal-ligand complexes and the protocols for obtaining crystals for X-ray diffraction that are reported herein are based upon his reports.

6. SYNTHESIS OF HETEROCYCLIC LIGANDS

There are several classical methods for preparing azobenzenes, the most important being the azo coupling reaction, the Wallach reaction and the Mills reaction. More recently, other synthetic methods such as the thermolysis of azides, has been developed.

Nevertheless, in the present work we use the azo coupling reaction because, in general, it gives high yields and short reaction times.

To synthesize compounds **1** and **4** aniline is reacted with the nitrosonium ion ($N{\equiv}O^+$) generated *in situ* from 10% HCl and $NaNO_2$. Once, the primary amine had reacted with $N{\equiv}O^+$, the subsequent protonation and deprotonation steps lead to the formation of the diazonium salt. Careful control of the pH to bellow pH 10 is important in order to prevent *N*-coupling reactions and the protonation of the amine which can reduce its reactivity.(17)

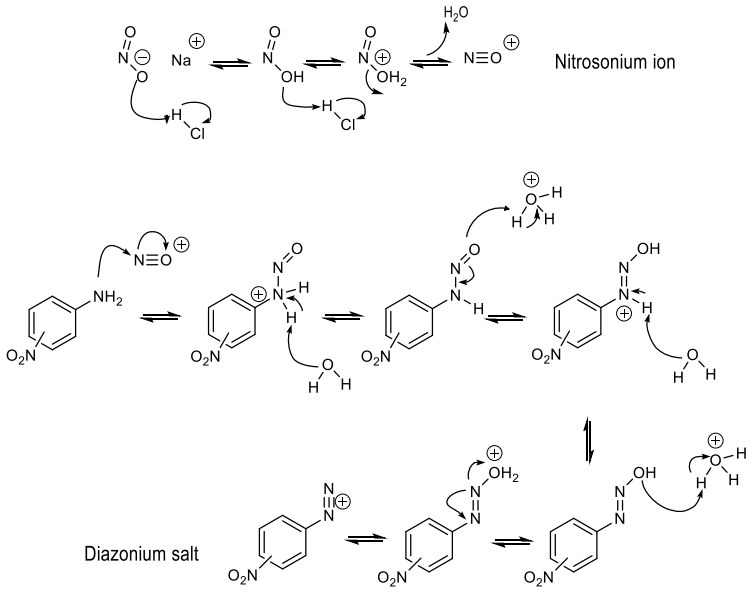

Scheme 1 Synthesis of diazonium salt(18)

It is also important to cool the reaction in an ice-water bath, because diazonium salts are usually unstable above 5 ºC. Although the diazotization reaction was discovered in the 1870s, it continues to be an active area of research today.(19)

In the electrophilic aromatic substitution (S_EAr) reaction of the diazonium salt with the phenol, substitution takes place preferentially at the *para*-position. If this position is blocked then substitution takes place at the *ortho*-position.(15)

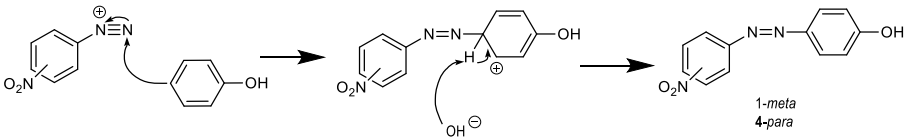

Scheme 2 Electrophilic aromatic substitution (S_EAr)

Once compounds **2** and **5** had been synthesized, the reduction of the nitro group was undertaken using the Zinin Reduction in which sulfide ion is the reducing agent. This reaction was first used in 1842 and since then has become a common and efficient method for the reduction of nitro groups. Mixtures of EtOH/water and or dioxane/water were employed in to dissolve the sodium sulfide and to prevent over-reduction.(20)

Since the nitro-compounds to be reduced incorporate an azo group, certain other common reduction methods, such as catalytic hydrogenation, would not be suitable. The activity of sodium sulfide as a reducing agent is based on the formation of $S_2O_3^{2-}$.

The stoichiometry of the reaction is as follows:(21-24)

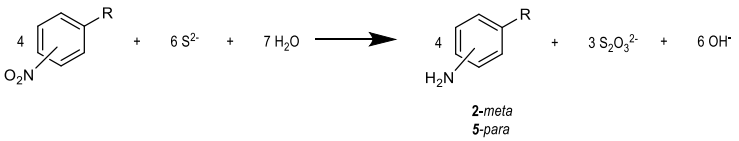

$$6OH^- + 2S^{2-} \rightarrow S_2O_3^{2+} + 3H_2O + 8e^-$$

$$6e^- + 4H_2O + RNO_2 \rightarrow RNH_2 + 6OH^-$$

Scheme 3 Mechanism of the Zinin Reaction

The equations above represent the theoretical conditions for the reduction, but often other side-reactions occur that can lead to low yields of the desired product.

The last reaction of the synthetic sequence is the formation of an imine or Schiff's base and is carried out in two steps. The first involves the attack of the amine at the carbonyl group of the aldehyde and must be carried out in a basic medium.

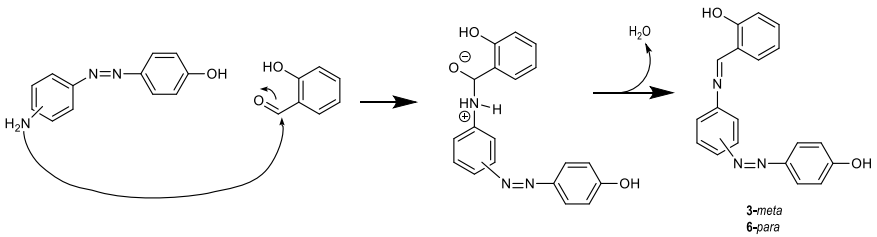

Scheme 4 Formation of Schiff's base[25]

7. RESULTS AND DISCUSSION

7.1. SYNTHESIS OF THE *META*-SUBSTITUTED LIGAND

The synthetic route for obtaining the *meta*-substituted ligand starts from 3-nitroaniline and is shown in **Scheme 5** below.

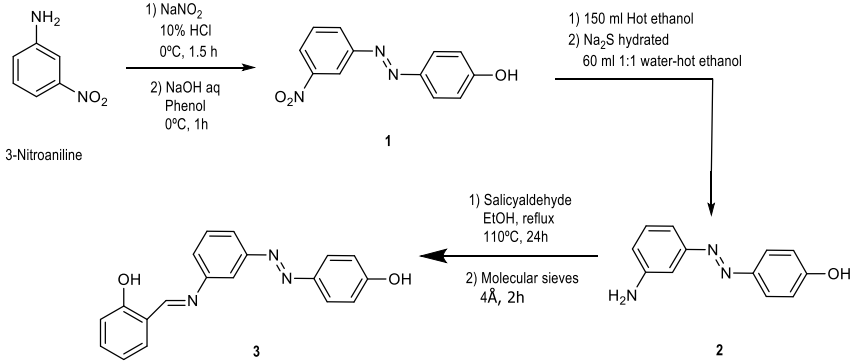

Scheme 5 Synthetic route to the *meta*-substituted ligand

7.1.1. Azo coupling reaction and S_EAr

The synthesis of nitro-compound **1** requires two steps. The first corresponds to the formation of the diazonium salt as described above in **Scheme 1**. The second, corresponds to the electrophilic aromatic substitution reaction in which phenol acts as a nucleophile and the diazonium salt acts as an electrophile (see **Scheme 2**).

Since the OH group in phenol is an electron donor and an *ortho/*para director the substitution reaction takes place in this position.

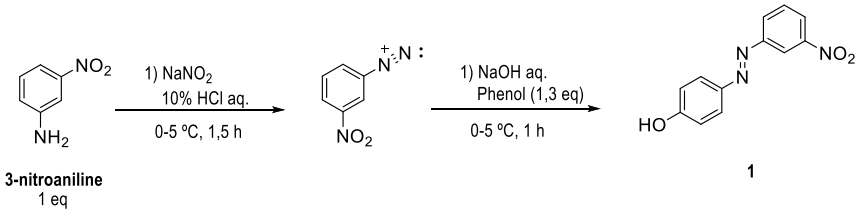

Scheme 6 Synthetic route to compound **1**

7.1.2. Reduction of the nitro group

The reduction of nitro-compound **1** to obtain the aniline **2** has been carried out as reported in the literature.(1)

Purification of the resulting crude-mixture was carried out by column chromatography on silica using dichloromethane as eluent.

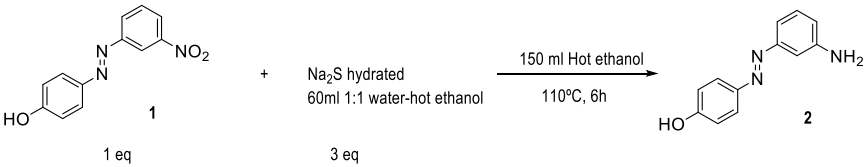

Scheme 7 Synthesis of aniline **2**

7.1.3. Condensation of the aniline with salicylaldehyde

The final reaction necessary for synthesizing the desired *meta*-substituted ligand was carried out by stirring a mixture of salicylaldehyde and compound **2** in absolute EtOH at reflux for 24 hours. After cooling the mixture was stirred with 4 Å molecular sieves at rt for 2 hours to remove any traces of water that might remain.

Since the desired *meta*-substituted ligand **3** is unstable to silica gel on account of it incorporating an imine group, it could not be purified by conventional column chromatography. This being so, the crude product was analyzed by ^{1}H-NMR spectroscopy and, if necessary was made to react with further quantities of salicylaldehyde or of compound **2** depending upon the state of the crude.

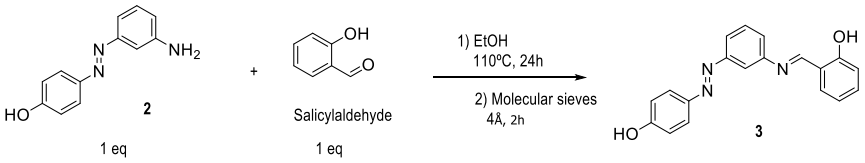

Scheme 8 Synthetic route to compound **3**

7.2. SYNTHESIS OF THE *PARA*-SUBSTITUTED LIGAND

The synthetic route for obtaining the *para*-substituted ligand is very similar to that used for the *meta*-substituted one and starts from 4-nitroaniline. (See **Scheme 9** below).

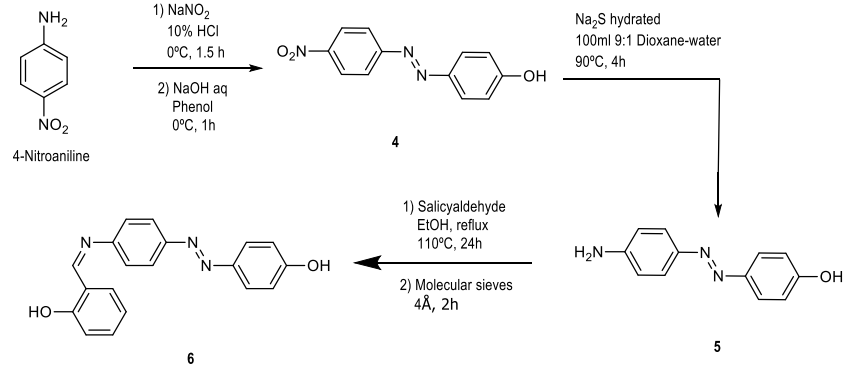

Scheme 9 Synthetic route to the *para*-substituted ligand

7.2.1. Azo coupling reaction and S_EAr

As in the case of the *meta*-substituted ligand, the synthesis of nitro-compound **4** requires two steps. The first corresponds to the formation of the diazonium salt as described above in **Scheme 1**. The second corresponds to the electrophilic aromatic substitution reaction in which phenol acts as a nucleophile and the diazonium salt acts as an electrophile (See **Scheme 2**).

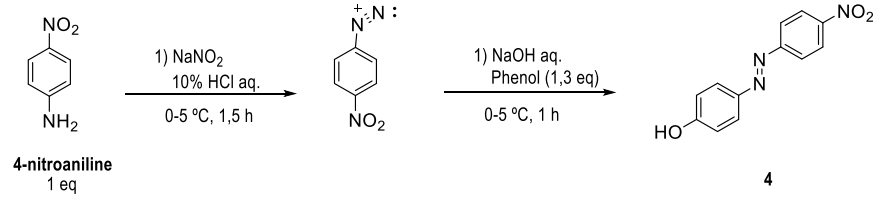

Scheme 10 Synthesis of compound **4**

7.2.2. Reduction of the nitro group

The reduction of the nitro-compound **4** to obtain aniline **5** was again carried out as reported in the literature,[26] using sodium sulphide and a mixture of dioxane and water. Purification of the resulting crude mixture was carried out by column chromatography on silica gel using dichloromethane as eluent.

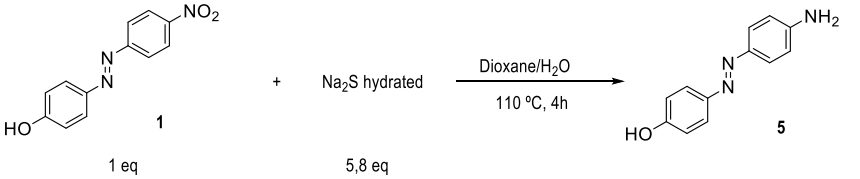

Scheme 11 Synthesis of compound **5**

7.2.3. Condensation of the aniline with salicylaldehyde

The final reaction necessary for synthesizing the desired *para*-substituted ligand was carried out by stirring a mixture of salicylaldehyde and compound **5** in absolute EtOH at reflux for 24 hours. After cooling the mixture was stirred with 4 Å molecular sieves at room temperature for 2 hours, to remove any traces of water that might remain.

Since the desired *para*-substituted ligand **6** is unstable to silica gel on account of it incorporating an imine group, it could not be purified by conventional column chromatography. This being so, the crude product was analyzed by ^{1}H-NMR spectroscopy and, if necessary, was made to react with further quantities of salicylaldehyde or compound **2** depending upon the state of the crude.

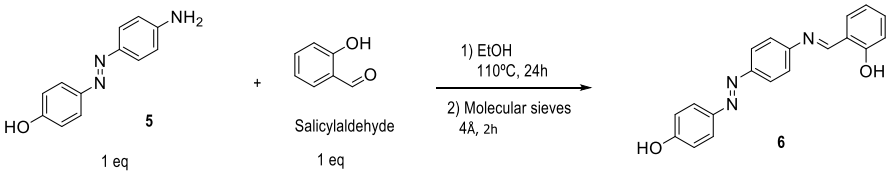

Scheme 12 Synthesis of compound **6**

7.3 COMPARISON OF THE SYNTHESES

In the case of both ligands, the formation of the diazonium salts and S_EAr reactions with phenol to yield compounds **1** and **4** were straightforward. The *meta*-substituted intermediate was obtained in a slightly higher yield (78%) than the *para*-substituted intermediate (66%).

On the other hand, the reduction of the nitro group to the amine in the case of intermediate **1** was more problematic than in the case of the corresponding reduction on the intermediate **4**. Careful control of the pH appears to be necessary, as is judicious choice of the solvent. Whereas the use of dioxane/water mixtures allowed the obtention of compound **5** in a sufficiently pure state to obviate the need for column chromatography, in the case of compound **2** this solvent system always led to an oily mixture of several compounds in which the desired intermediate was only a minor component. Changing the solvent to an ethanol/water mixture and extending the reaction by 2 hours gave much better results, although the produce was still somewhat impure.

The condensation reaction of the aniline with salicylaldehyde was straightforward in both cases.

7.4 ATTEMPTED SYNTHESIS OF A LIGAND INCORPORATING TWO AZO GROUPS

The objective was to obtain an extended chain linear compound incorporating two azo groups for metal-ion coordinating and with a phenol at either end.

Treatment of aniline **5,** previously synthesized by Javier González,[15] with 10% HCl and NaNO2 at 0 ºC gave the corresponding diazonium salt. It was the reasoned that reaction of this salt with resorcinol would then furnish the desired extended ligand **7** (See **Scheme 13**).

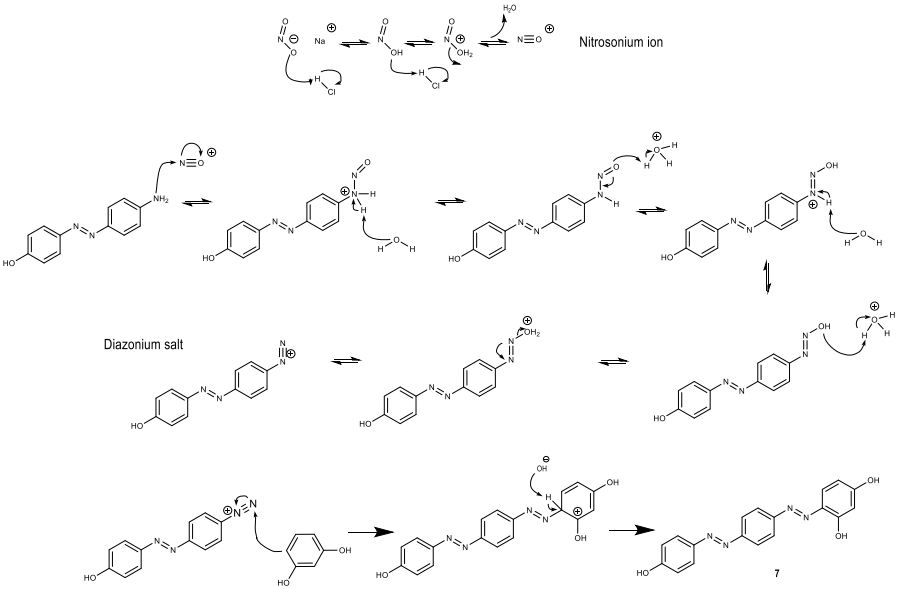

Scheme 13 Synthesis of compound **7**

TLC of the crude reaction mixture showed that all reactant had been consumed and that two products were formed. ^{1}H-NMR spectroscopy in MeOD of the crude reaction mixture showed four peaks that integrated to 2 protons but that are not consistent with the structure of amine **5** nor of the desired product **7** (See Appendix).

The components of the mixture were separated by column chromatography on silica gel, using a mixture of 95:5 CH_2Cl_2/MeOH as eluent. However, mass spectrometry of both components indicated that neither were the amine **5** nor the desired product **7**.

7.5 STUDY OF THE COORDINATION WITH METAL CATIONS

Experiments on the coordination with metal ions have been carried out with ligand **3** in order to compare the results obtained with those with ligand **6**.

Initially, it was conjectured that metal ions might coordinate to these ligands in different ways: by interaction with the terminal phenol group, by interaction with the π bond of the azo group or by interaction with the imine nitrogen atom and the hydroxyl group of salicylaldehyde.

X-ray crystallography demonstrates that coordination of the metal ion occurs by the third of these options, that is to say, by interaction with the nitrogen of the imine and the hydroxyl group of the salicylaldehyde.

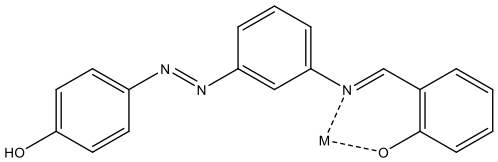

Fig 6 Possible location of metal coordination

Coordination assays were carried out with the acetates of zinc, copper and cobalt. The procedure consisted of treatment of ligand **3** with the desired metal and a base (TBAOH). The solvent used for the reaction was MeOH and, before closing the vials, *n*-hexane and diethyl ether were added. *n*-Hexane inhabits the crystallization process and, since methanol and hexane are not miscible, diethyl ether was added as co-solvent. Crystallization was then induced by slow evaporation.

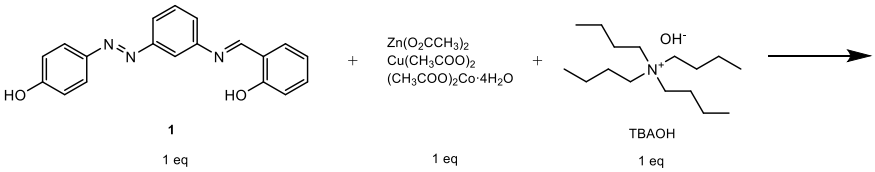

Scheme 14 Procedure for crystallization

7.5.1. X-ray Crystal Structure Determinations

The structures of the free *para*-substituted ligand **6** (AZO**1**) synthesized by Javier González, together with that of its zinc-complex synthesized by Diego Abad[25] and the copper-complexed *meta*-substituted ligand **3** (AZO**2**) have been studied by X-ray diffraction in order to determine their exact structures. Furthermore, the crystals of the free *meta*-substituted ligand, together with all of the others mentioned previously will be sent to the ALBA Synchrotron in order to study their

structures more closely. This is necessary because the crystals obtained in this work are not of high quality. A crystal may be considered to be of good quality if it has an R-Factor (%) of less than 10%. However, those obtained in this project have values greater than this threshold.

Another indication of the relatively low quality of the crystals was that, on attempting to present the X-ray structures in the Mercury software "Elipsoid Style" it was seen that not all atoms were represented as perfect spheres. This mode of the software shows the thermal motion of the atoms and the fact that not all atoms appeared as perfect spheres indicated that there was an error in the position of the atoms while the measurements were being made.

The crystal structure images shown below are represented using the Mercury software "Capped Style". The structure of the free *para*-substituted ligand is shown in **Figure 7**, and corroborates the initial idea that compounds with this substitution pattern are more stable. It can be seen that a molecule of H_2O is situated between two molecules of the ligand and forms hydrogen bonds to the hydroxyl groups of their phenols.

Fig 7 Crystal structure of ligand **6** (AZO**1**)

Bond distances and angles are shown in **Table 1**. In the case of the azo and imine bonds, these distances are usually between 1.2 Å and 1.3 Å, respectively and, as can be seen, these are in broad agreement with the experimentally obtained values. The dispersion in values is due to the low quality of the crystals.

Table 1. Selected Bond Distances (Å) and Angles (deg) for compound **6**			
C(7)-N(1)-C(8)	119.8(7)	C(33)-N(6)-N(5)	114.1(7)
C(11)-N(2)-N(3)	115.1(7)	C(27)-N(4)-C(26)	118.3(7)
C(14)-N(3)-N(2)	113.1(7)	C(30)-N(5)-N(6)	117.4(7)
C(7)-N(1)	1.30(1)	N(2)-N(3)	1.24(1)
C(26)-N(4)	1.30(1)	N(5)-N(6)	1.22(1)

The zinc complex [Zn(azo1)$_2$], was also obtained in crystalline form and its X-ray structure is shown below in **Figure 8**. The structure of this complex is reported in more detail in parallel studies.[25]

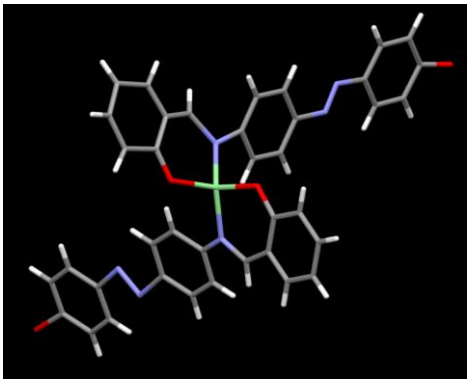

Fig 8 Crystal structure of zinc-complexed ligand [Zn(azo1)$_2$][25]

The following table (**Table 2**) presents a summary of the characteristics of the different crystals obtained.

Table 2. Structural Characteristics of the three synthetised crystals			
	AZO1	**$[Zn(azo_1)_2]$**	**$[Cu_4(OMe)_2(AcO)_4(azo_2)_2]$**
Empirical formula	$C_{19}\ H_{16}\ N_3\ O_{2.5}$	$C_{19.5}\ H_{14.25} N_3\ O_{2.75}\ Zn_{0.5}$	$C_{19}\ H_{15}\ Cu\ N_3\ O_2$
Space group	$P\bar{1}$	P1	P21
Cyst syst	triclinic	triclinic	orthorhombic
a/Å	6.0468(10)	8.3143(9)	17.9808(13)
b/Å	7.1184(9)	10.6621(12)	9.3709(7)
c/Å	36.266(5)	19.400(2)	28.325(2)
α/deg	88.275(9)	98.597(9)	90
β/deg	88.456(11)	97.281(8)	90
γ/deg	89.744(11)	97.196(8)	90
V/ Å3	1559.73	1668.4	4772.66
Z	4	4	12
Z'	2	4	6
D/g cm-3	1.390	1.462	1.590
T/K	100	100	100
R-Factor (%)	14.4	16.7	9.47
Packing coefficient	0.714286	0.69949	0.686793

7.5.2. $[Cu_4(OMe)_2(AcO)_4(azo_2)_2]$ (8)

In this work reported here, the only crystal obtained to date is the tetrameric copper complex, $[Cu_4(OMe)_2(AcO)_4(azo_2)_2]$ (**8**). This structure consists of two azo ligands chelating to the copper ions as shown in **Figure 6**. It consists of 4 copper ions that have different coordination numbers. Both Cu(1) and Cu(4) have square-planar geometries (NC=4), while Cu(2) and Cu(3) exhibit distorted octahedral geometries (NC=6).

As can be seen in **Figure 9**, the cluster is composed not only of copper ions and the ligands themselves but also of methoxide ions (in red). These act as bridging ligands between three copper ions giving rise to a Defective Double QD. Methanol molecules bonded to the methoxide ions can also be observed and these are known as "non-innocent solvent" molecules. Such a phenomenon is common when methanol is used as solvent in such crystallization protocols.

The cluster has the form of a cube in which two vertices have been lost, such that it is not completely closed. Also noteworthy is the fact that the azo groups are orientated in opposite directions.

A curious characteristic of the obtained crystal is that all copper ions in the structure are Cu^{2+} whereas normally both Cu^{+} and Cu^{2+} are found.

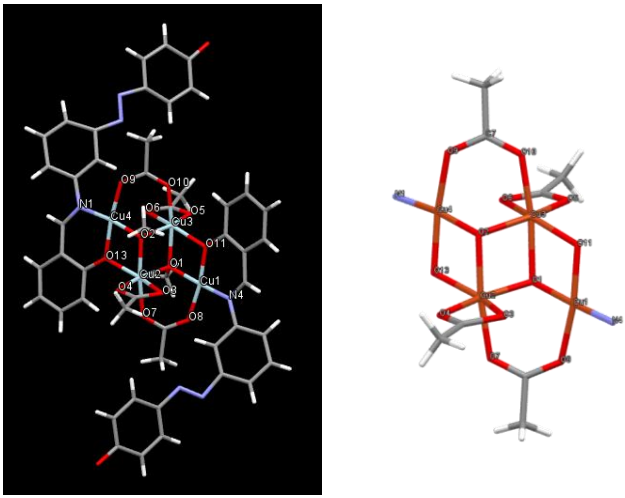

Fig 10 Crystal structure of $[Cu_4(OMe)_2(AcO)_4(azo_2)_2]$ (**8**)

If the bond angles around Cu(2) and Cu(3) are considered to be practically identical, as are those around Cu(4) and Cu(1) then a list of characteristic bond angles can be drawn up. (See **Table 3**). In the case of a square planar geometry the bond angles should be 90º, the same value that would be expected in the case of an octahedral geometry. The observed values deviate somewhat from this ideal, particularly so in the case of the octahedral geometry, because the octahedron is distorted.

Table 3. Selected Bond Distances (Å) and Angles (deg) for compound **8**

N(4)-Cu(1)-O(8)	94.3(7)	O(3)-Cu(2)-O(4)	56.9(6)
N(4)-Cu(1)-O(1)	176.4(7)	O(3)-Cu(2)-O(7)	85.6(6)
Cu(1)-O(1)-Cu(3)	103.2(6)	O(13)-Cu(2)-O(1)	95.0(6)
Cu(1)-N(4)	1.97(2)	Cu(2)-O(4)	1.95(1)
Cu(1)-O(11)	1.86(1)	Cu(2)-O(3)	2.57(1)

It can be seen that, in the unit cell of the crystal obtained, the atoms are placed such that they form a type of spike

If the unit cell is represented using the “Symmetry operation” mode of the software in which each atom has a color according to the symmetry relationship it has with the asymmetric unit, two symmetry operators may be observed as seen in **Table 4**.

Table 4. Symmetry Operators List

Color	Symm. Op.	Description	Order	Type
Grey	x, y, z	Identity	1	1
Green	-x, ½ + y, -z	Screw axis (2-fold)	2	2

The only symmetry operator that has every molecule has is that of identity and does not require a symmetry element. On the other hand, the screw axis combines rotation and translation symmetry elements.

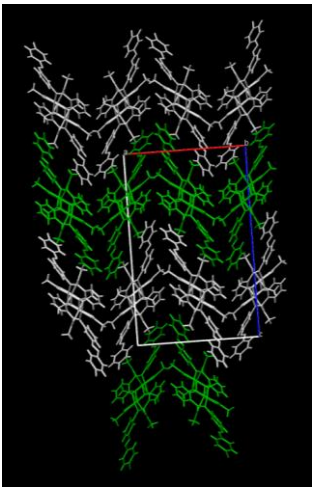

Fig 11 Representación de la celda unidad

The structure also shows that a single equivalent of base is not sufficient to fully deprotonate the phenol hydroxyl group. This could be remedied by using more than one equivalent of TBAOH or by using a stronger base.

7.6 *CIS/TRANS* ISOMERIZATION OF THE *META*-SUBSTITUTED LIGAND (3)

Since an experimental study of the absorption spectra of the *meta*-substituted ligand was not an objective of this work, theoretical calculations that simulate the absorption spectra of this ligand were carried out by Drs. Jordi Cirera and Jorge Echevarría (Inorganic Chemistry Section, IQTC UB).

According to their calculations $\Delta G_{cis/trans}$ for the *meta*-substituted ligand is -15.45 kcal/mol. This is a relatively high value and indicates that the *trans*- form is more stable than the *cis*- form. The calculations were carried out by simulating irradiation at a wavelength of 430 nm for 10 min.

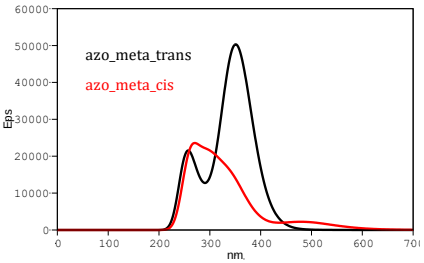

Fig 12 Theoretical *cis/trans* isomerization

8. EXPERIMENTAL SECTION

8.1. MATERIALS AND METHODS

Nuclear magnetic resonance spectroscopy (NMR)

^{1}H and ^{13}C-NMR spectra were recorded on a Varian Mercury 400MHz instrument, in $CDCl_3$ and DMSO containing 0.03% (v/v) of TMS as internal standard. Coupling constants (J) are given in Hz and chemical shifts are reported in ppm (δ). To prepare the samples, 5-10 mg (in the case of ^{1}H-NMR spectra) or 25-30 mg (in the case of ^{13}C-NMR spectra) of the compound were dissolved in 0,7 mL of the deuterated solvent. NMR spectra were analyzed using MestReNova software.

Infrared spectroscopy (IR)

IR spectra were recorded at rt (20-25 ºC) on a Varian Nicolet 6700FT-IR instrument and analyzed with Omnic software.

Thin layer chromatography (TLC)

TLC was carried out on aluminum sheets of a thin layer of silica gel (60F, 0,2 mm). Plates were visualized under UV light.

X-ray crystal structure determination

X-ray crystal structures were obtained using a Bruker Apex II Smart Quazar diffractometer the data were treated using the Mercury software package available from the Cambridge Data Base.

8.2. PREPARATION OF THE *META*-SUBSTITUTED HETEROCYCLIC LIGAND

8.2.1. Synthesis of 4-((3-nitrophenyl)diazenyl)phenol (1)

A mixture of 3-nitroaniline (3,984g, 28,86 mmol) in 10% HCl (70 mL) was stirred at rt in a round bottomed flask and the resulting solution was paced in an ice-water bath. A solution of

$NaNO_2$ (2,613g, 37,87 mmol) in water (60 mL) was added dropwise over 90 min, with continual stirring. A mixture of phenol (3.494 g, 37.13 mmol) and NaOH (1.613 g, 40.32 mmol) in water (40 mL) was then added dropwise over 60 min maintaining the ice-water bath. The mixture was then stirred for an additional 3 hours at the same temperature. The mixture was allowed to attain rt and stirred overnight. The resulting brown precipitate was filtered and dried at rt.

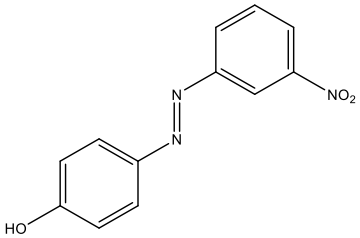

Brown solid. Yield: 78% (5.50 g). TLC: (CH_2Cl_2 95:5 MeOH) Rf=0.81. **^{1}H-NMR** (400 MHz, $CDCl_3$): δ=8.70 (t, J = 8.7 Hz, 1H), 8.25 (dd, J= 8.25 Hz, 2H), 7.93 (d, J = 7.93 Hz, 2H), 7.68 (t, J=7.68 Hz, 1H), 6.98 (d, J=6.98 Hz, 2H). **^{13}C-NMR** (400 MHz, $CDCl_3$): δ=184, 158, 147, 138, 129.84, 129.01, 125, 124, 116.71, 116.01. **IR (cm^{-1})**: 3084, 1604, 1587, 1522, 1504

8.2.2 Synthesis of 4-((3-aminophenyl)diazenyl)phenol (2)

Hydrated Na_2S 7.419 g (95.06 mmol) was dissolved in 50 ml of a 1:1 mixture of water-hot ethanol until complete dissolution. This solution was poured into a solution of the compound **1** (2.519 g, 10.36 mmol) in 150 ml of hot EtOH. The mixture was refluxed at 110 ºC for 6 hours and then stirred overnight. After cooling, the mixture was extracted with AcOEt (5 x 30 mL). The organic layers were combined, dried over $MgSO_4$ and filtered. Then resulting solution was concentrated under vacuum to obtain an orange oil.

Purification by column chromatography (silica gel, CH_2Cl_2) yielded an orange solid.

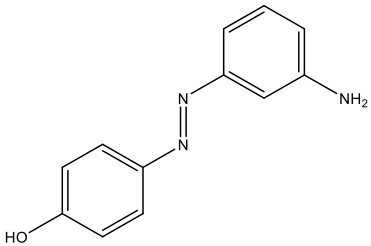

Orange solid. Yield: 55% (0.392 g). TLC: (CH_2Cl_2 95:5 MeOH) Rf=0.62. **^{1}H-NMR** (400 MHz, $CDCl_3$): δ=7.86 (d, J = 7.86 Hz, 2H), 7.30 (t, J= 7.30 Hz, 2H), 7.18 (s, 1H), 6.94 (d, J=6.94 Hz, 2H), 6.78 (dt, J=6.78 Hz, 1H), 5,30 (s, 2H). **^{13}C-NMR** (400 MHz, $CDCl_3$): δ=160.97, 150.02, 145.69, 129.89, 124.96, 116.30, 112.34, 105.67. **IR (cm^{-1})**: 3359, 2918, 2850, 1582, 1503

8.2.3 Synthesis of 2-((3-((4-hydroxyphenyl)diazenyl)phenyl)imino)methyl)phenol (3)

Salicylaldehyde 0.117 g (0.958 mmol) was added to a solution of the compound **2** (0.199 g, 0.934 mmol) in EtOH (25 ml) and the resulting mixture was heated at reflux for 24 hours. After

cooling to rt, 4 Å molecular sieves were added and the mixture gently for 2 hours. The solution was filtered and concentered under vacuum to give an orange solid.

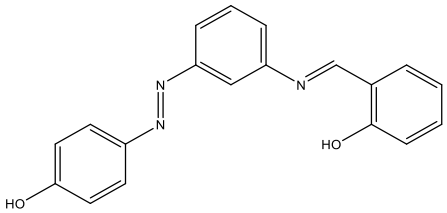

Orange solid. Yield: 93% (0.276 g). TLC: (CH_2Cl_2 95:5 MeOH) Rf=0.64 **^{1}H-NMR** (400 MHz, $CDCl_3$): δ=8.74 (s, J = 8.74 Hz, 1H), 7.90 (d, J= 7.90 Hz, 2H), 7.81 (t, J = 7.81 Hz, 2H), 7.56 (t, J=7.56 Hz, 1H), 7.43 (m, J=7.43 Hz, 3H), 7.06 (d, J=7.06, 1H), 6.98 (t, J=6.98 Hz, 3H). **^{13}C-NMR** (400 MHz, $CDCl_3$): δ=164.85, 161.68, 160.73, 155.18, 153.56, 149.71, 145.60, 143.25, 134.00, 133.14, 130.76, 125.48, 124.10, 121.31, 119.71, 117.08, 116.45, 114.50. **IR (cm^{-1})**: 2546, 1622, 1605, 1584, 1138

8.3. PREPARATION OF THE PARA-SUBSTITUTED HETEROCYCLIC LIGAND

8.3.1. Synthesis of 4-((4-nitrophenyl)diazenyl)phenol (4)

A mixture of 4-nitroaniline (4.008 g, 29.02 mmol) in 10% HCl (70 mL) was stirred at rt in a round bottomed flask and the resulting solution was introduced into an ice-water bath. A solution of $NaNO_2$ (2.582 g, 37,42 mmol) in water (60 mL) was added dropwise for 90 min, with continual stirring. A mixture of phenol (3.524 g, 37.44 mmol) and NaOH (1.542 g, 38.55 mmol) in water (40 mL) was then added dropwise over 60 min maintaining the ice-water bath. The mixture was then stirred for an additional 3 hours at the same temperature. The mixture was allowed to attain rt and stirred overnight. The resulting brown precipitate was filtered and dried at rt.

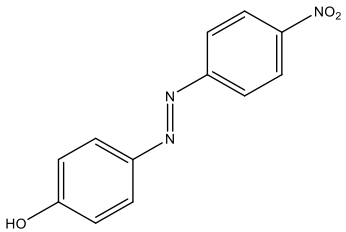

Brown solid. Yield: 64% (4.534 g). TLC: (CH_2Cl_2 95:5 MeOH) Rf=0.78. **^{1}H-NMR** (400 MHz, $CDCl_3$): δ=8.37 (d, J = 8.37 Hz, 2H), 7.96 (dd, J= 7.96 Hz, 4H), 6.98 (d, J = 6.98 Hz, 2H) **IR (cm^{-1})**: 3369, 1603, 1685, 1503

8.3.2 Synthesis of 4-((4-aminophenyl)diazenyl)phenol (5)

Hydrated Na_2S 1.516 g (19.09 mmol) was dissolved in 90 mL of dioxane and 10 mL of water until complete dissolution. This solution was poured into a solution of the compound **4** (0.805 g, 3.3 mmol). The mixture was refluxed at 110 ºC for 4 hours and then stirred overnight. After cooling, the mixture was transferred to a separatory funnel (250 mL), neutralized with 100 mL of $NaHCO_3$ (sat) and 20 mL of NaCl (sat) in the same funnel and extracted with CH_2Cl_2 (5 x 100 mL). The organic layers were combined, dried over $MgSO_4$ and filtered. Then resulting solution was concentrated under vacuum to obtain an orange oil.

Purification by column chromatography (silica gel, CH_2Cl_2) yielded an orange solid.

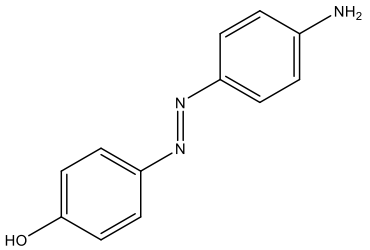

Orange solid. Yield: 55% (0.392 g). TLC: (CH_2Cl_2 95:5 MeOH) Rf=0.60. **^{1}H-NMR** (400 MHz, $CDCl_3$): δ=8.70 (t, J = 8.70 Hz, 1H), 8.25 (dt, J= 8.25 Hz, 2H), 7.94 (d, J=7.93, 2H), 7.68 (t, J=7.68 Hz, 1H), 6.98 (d, J=6.98 Hz, 2H) **IR (cm^{-1})**: 3340, 2916, 2848, 1597, 1586

8.3.3 Synthesis of 2-((4-((4-hydroxyphenyl)diazenyl)phenyl)imino)methyl)phenol (6)

Salicylaldehyde 0.137 g (1.12 mmol) was added to a solution of the compound **5** (0.214 g, 1.005 mmol) in EtOH (25 ml) and the resulting mixture was heated at reflux for 24 hours. After cooling to rt, 4 Å molecular sieves were added and the mixture gently for 2 hours. The solution was filtered and concentered under vacuum to give an orange solid.

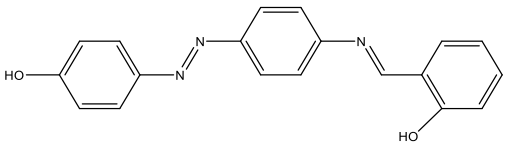

Red solid. Yield: 94% (0.201 g). TLC: (CH_2Cl_2 95:5 MeOH) Rf=0.62. **^{1}H-NMR** (400 MHz, $CDCl_3$)): δ=7.77 (dd, J=7.78, 4H), 6.92 (d, J=6.92, 2H), 6.74 (d, J=6.74, 2H) plus small peaks corresponding to salicylaldehyde.

8.4. COMPLEXATION OF LIGANDS WITH METALS

In order to prepare the ligand complexes with metal ions the procedure used were those previously employed by Javier González[15] and Diego Abad.[16]

8.4.1 Complexation of AZO2 with Zn

$Zn(O_2Ac)_2$ (0.029 g, 0.16 mmol) was dissolved in 10 mL of MeOH in an Erlenmeyer flask and 0.050 mg (0.16 mmol) of ligand **3** (AZO**2**) was added. 41.74 µL (0.16 mmol) of TBAOH was added and the mixture was stirred at rt for 1 hour. After filtration the orange solution was placed in a vial and 5 mL of *n*-hexane and 5 mL of diethyl ether were added and the vial was closed.

8.4.2 Complexation of AZO2 with Cu (8)

$Cu(AcO)_2$ (0.029 g, 0.16 mmol) was dissolved in 10 mL of MeOH in an Erlenmeyer flask and 0.050 mg (0.16 mmol) of ligand **3** (AZO**2**) was added. 41.74 µL (0.16 mmol) of TBAOH was added and the mixture was stirred at rt for 1 hour. After filtration the brown-green solution was placed in a vial and 5 mL of *n*-hexane and 5 mL of diethyl ether were added and the vial was closed.

8.4.3 Complexation of AZO2 with Co

$(AcO)_2Co{\cdot}4\ H_2O$ (0.029 g, 0.16 mmol) was dissolved in 10 mL of MeOH in an Erlenmeyer flask and 0.050 mg (0.16 mmol) of ligand **3** (AZO**2**) was added. 41.74 µL (0.16 mmol) of TBAOH was added and the mixture was stirred at rt for 1 hour. After filtration the red solution was placed in a vial and 5 mL of *n*-hexane and 5 mL of diethyl ether were added and the vial was closed.

8.4.4 Complexation of AZO2 with Zn

$Zn(O_2Ac)_2$ (0.029 g, 0.16 mmol) was dissolved in 10 mL of MeOH in an Erlenmeyer flask and 0.050 mg (0.16 mmol) of ligand **3** (AZO**2**) was added. 41.74 µL (0.16 mmol) of TBAOH was added and the mixture was stirred at rt for 1 hour. After filtration the orange solution was placed in a vial and 5 mL of *n*-hexane were added and the vial was closed.

9. CONCLUSIONS

The synthesis of the desired *meta* and *para*-substituted ligands has been accomplished. Nevertheless, the reduction of the nitro group to the corresponding aniline is operationally tedious and gives rather low yields, especially in the case of the *meta*-substituted-compound. If further quantities of these ligands are required in the future, this reaction needs to be optimized or changed in favor of a cleaner, higher yielding procedure.

Studies of the coordination of these ligands with metal cations have been initiated ant a tetrameric Cu has already been isolated and subjected to X-ray crystallography. Attempts at complex formation with other metal cations have, so far, not yielded crystals. It should be pointed out here that such crystallizations may require weeks or even months in order to yield crystals that are suitable for X-ray diffraction.

The synthesis of the ligand incorporating two azo groups did not yield the desired product and attempts to deduce the structure of the product formed, so far, been unsuccessful. Future work in our group will be directed towards elucidating the structure of this compound and towards synthesizing the desired product.

10. REFERENCES AND NOTES

Cârlescu, I.; Scutaru, A. M.; Apreutesei, D.; Alupei, V.; Scutaru, D. The liquid crystalline behaviour of ferrocene derivatives containing azo and imine linking groups, *Liq. Cryst*. **2007**, *34*, 775-785, DOI: 10.1080/02678290701343190

2. Valizadeh, H.; Shomali, A.; Ghorbani, J.; Noorshargh, S. Synthesis of a nitrite functionalized star-like poly ionic compound as a highly efficient nitrosonium source and catalyst for the diazotization of anilines and subsequent facile synthesis of azo dyes under solvent-free conditions, Dyes Pigm. **2015**, *177*, 64-65, DOI: 10.1016/j.dyepig.2015.02.007
3. Piquer, L. Sañudo, E. C. Heterometallic 3d-4f single-molecule magnets. Dalton Trans. **2007**. *44*, 8771-8780. DOI: 10.1039/c5dt00549c
4. Bogani, L.; Wernsdorfer, W. Molecular spintronics using single-molecule magnets. Nanosci. Technol. **2009**, *7*, 194-201. DOI: 10.1142/9789814287005_0020
5. Milburn, G. J.; Woolley, M. J. Quantum nanoscience. Contemp. Phys. **2008**, *49*, 413-433. DOI: 10.1080/00107510802601724
6. Friedman, J. R.; Sarachik, M. P.; Tejada, J.;Ziolo, R. Macroscopic measurement of resonant magnetization tunneling in high-spin molecules. Phys. Rev. Lett. **1996**, *76*, 38303833. DOI: 10.1103/physrevlett.76.3830
7. Sessoli, R.; Gatteschi, D.; Caneschi, A.: Novak, M. A.. Magnetic bisability in a metal-ion cluster. Nature **1996**, *365*, 141-143. DOI: 10.1038/365141a0
8. Christou, G.; Gatteschi, D.; Hendrickson, D. N.; Sessoli, R. Single-molecule magnets. MRS Bull. **2000**, *25*, 66-71. DOI: 10.1557/mrs2000.226
9. Woodruff, D. N.; Winpenny, R. E. P.;Layfield, R.A. Lanthanide single-molecule magnets. Chem. Rev. **2013**, *113*, 5110-5148. DOI: 10.1021/cr400018q
10. Guo, F. -S.; Day, B. M.; Chen, Y.; Tong, M. L.; Mansikkamäki, A.; Layfield, R. A. Magnetic hysteresis up to 80 kelvin in a dysprosium metallocene single-molecule magnet. Science **2018**, *362*, 1400-1403. DOI: 10.1126/science.aav0652
11. Tecilla, P.; Bonifazi, D. Configurational selection in azobenzene-based supramolecular systems through dual-stimuli processes. ChemistryOpen **2020,** *9*, 529-544. DOI: 10.1002/open.202000045
12. Fihey, A.; Perrier, A.; Browne, W. R.; Jacquemin, D. Multiphotochromic molecular systems. Chem. Soc. Rev. **2015**, *44*, 3719-3759. DOI: 10.1039/c5cs00137d
13. Liu, J.; Bu, W.; Pan, L.; Shi, J. NIR-Triggered anticancer drug delivery by upconverting nanoparticles with integrated azobenzene-modified mesoporous silica. Angew. Chem. Int. Ed. **2013,** *125*, 4471–4475. DOI: 10.1002/anie.201300183
14. Boulahfa, A. Synthesis of azo-imina compounds able to coordinate metallic cations. Treball final de màster .**2020**, Universitat de Barcelona. Facultad de Química. Barcelona.
15. González, J. Synthesis of new azo/imine ligands and study of it's complexation with cations. Treball final de grau. **2021**, Universitat de Barcelona. Facultad de Química. Barcelona.
16. Abad, D. Synthesis of new azo/imine ligands and study of it's complexation with cations. Treball final de grau. **2021**, Universitat de Barcelona. Facultad de Química. Barcelona.
17. Merino, E. Synthesis of azobenzenes: the coloured pieces of molecular materials. Chem. Soc. Rev. **2011**, *40*, 3835. DOI: 10.1039/c0cs00183j
18. Ashenhurst, J. Reactions of diazonium salts: Sandmeyer and related reactions. Master Organic Chemisty. Recovered May 9th, 2021 of https://www.masterorganicchemistry.com/2018/12/03/reactions-

of-diazonium-salts-sandmeyer-and-related-reactions/#:~:text=Mechanism%3A%20Formation%20of%20Diazonium%20Ions,-Formation%20of%20nitrosonium&text=The%20first%20key%20reagent%20for,nitrous%20acid%20(HNO2).&text=The%20key%20purpose%20of%20HCl,that%20forms%20the%20diazonium%20salt. (March 4th, 2021).

19. Liljenberg, M. Quantum chemical studies of aromatic substitution reactions. KTH Chemical Science and Engineering, Royal Institute of Technology, Sweden, 2017
20 Groggins, P. H. Unit processes in organic synthesis, McGraw-Hill, 1958
21. Cope, O. J; Brown, R. K. The reduction of nitrobenzene by sodium sulphide in aqueous ethanol. Can. J. Chem. **1961**, *39*, 1695-1710, DOI: 10.1139/v61-217
22. Hashimoto, S.; Sunamoto, J. The alkaline sulfide reduction of aromatic nitro compounds. VIII. The correlation between sodium monosulfide and hydrosulfide in the reduction of sodium m-nitrobenzene sulfonate. Bull. Chem. Soc. Jpn. **1966**, *39*, 1207-1211. DOI: 10.1246/bcsj.39.1207
23. Porter, H.K. The Zinin reduction of nitroarenes. Org. React. **2011**, *20*, 4555-481. DOI: 10.1002/0471264180.or020.04
24. Mondal, U.; Puthankot, A.; Sen, S.; Singh, G. Novelties of triphasic phase transfer catalysed Zinin reduction of nitrochlorobenzene by H2S-laden monoethanolamine. RSC Adv. **2016**, *6*, 23666-23676. DOI: 10.1039/c5ra26856g
25. Cordes, E. H.; Jencks, W. P. On the mechanism of Schiff base formation and hydrolysis. J. Am. Chem. Soc. **1962**, *84*, 832-837. DOI: 10.1021/ja00864a031
26. Zhou, D.; Wang, Y.; Jia, J.; Yu, W.; Qu, B.; Li, X.; Sun, X. (2015). H-bonding and charging mediated aggregation and emission for fluorescence turn-on detection of hydrazine hydrate. Supporting information. ChemComm. **2015**, *51*, 10656-10659. DOI: 10.1039/c5cc02897c
27. Bip.weizmann.ac.il. Symmetry operation colouring. [online]. Recovered June 9th, 2021 of https://bip.weizmann.ac.il/course/structbioinfo/databases/CCDC_Mercury/mercury.3.73.html#319047

11. ACRONYMS

IR	Infrared
NIR	Near infrared
NMR	Nuclear magnetic resonance
QTM	Quantum tunnelling of magnetization
Rf	Retention factor (TLC)
rt	Room temperature
SMMs	Single molecules magnet
TBAOH	Tetra-*n*-butylammonium hydroxide
TLC	Thin layer chromatography
UV	Ultraviolet-visible

APPENDICES

APPENDIX 1: NMR SPECTRA

COMPOUND 1

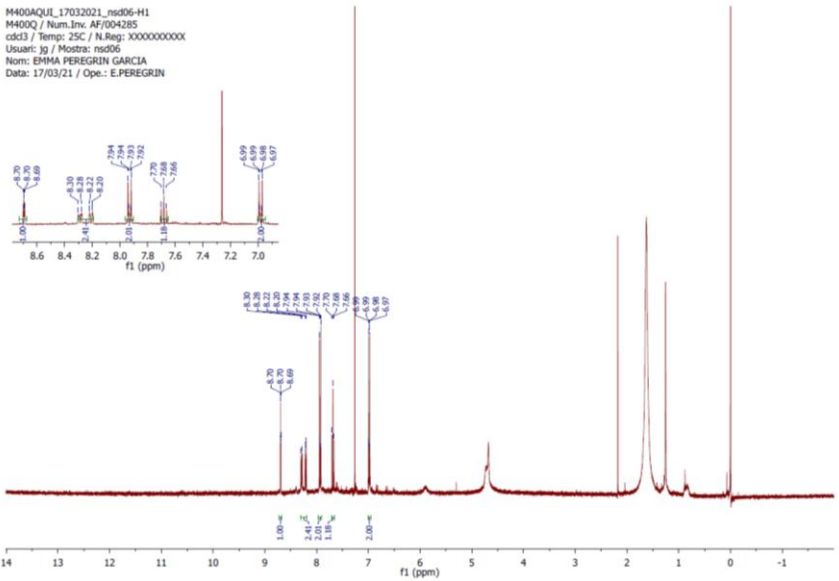

Fig 1 ^{1}H-NMR compound **1**

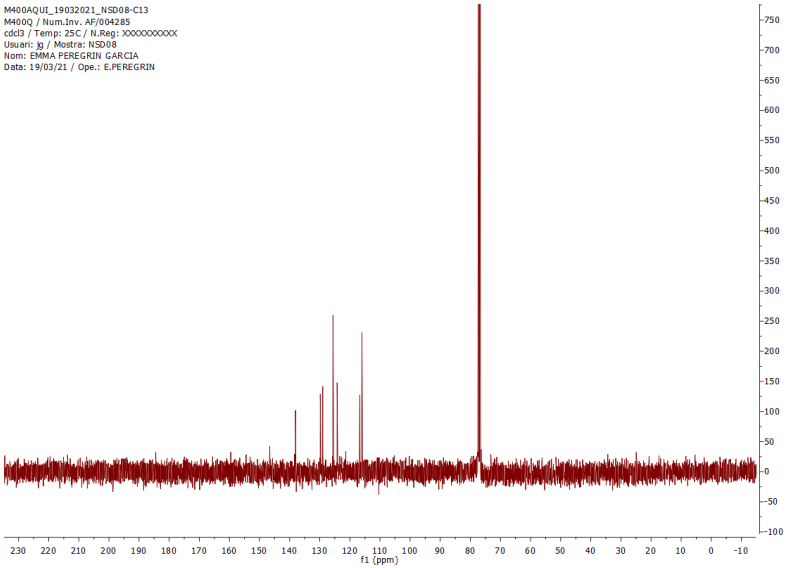

Fig 2 ^{13}C-NMR compound **1**

COMPOUND 2

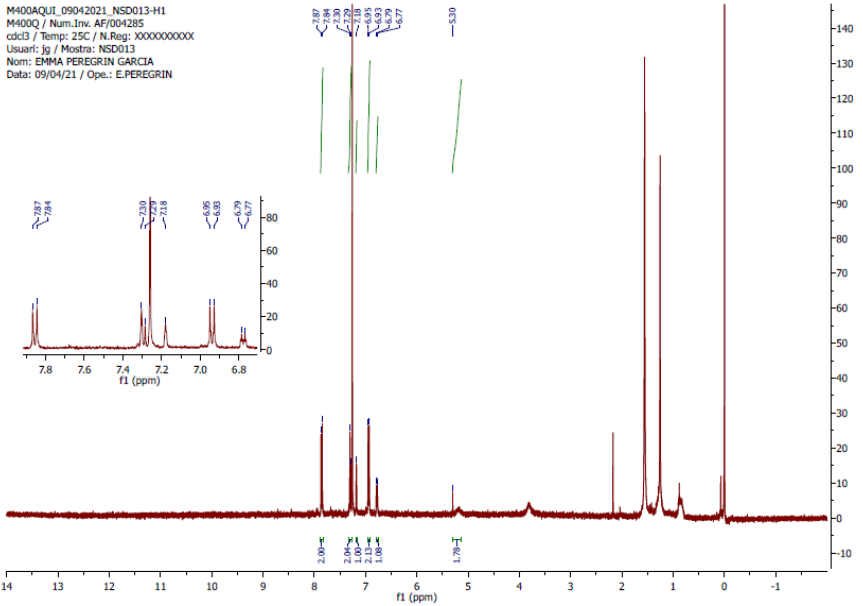

Fig 3 ^{1}H-NMR compound **2**

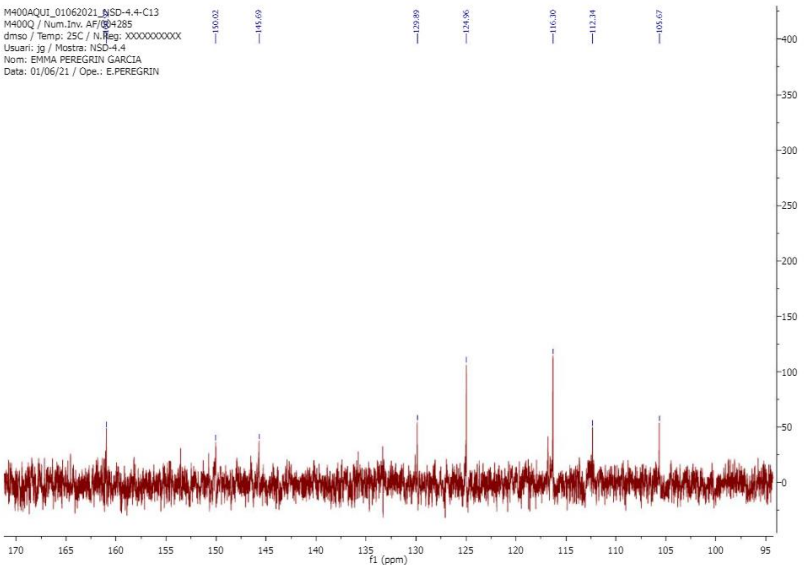

Fig 4 ^{13}C-NMR compound **2**

COMPOUND 3

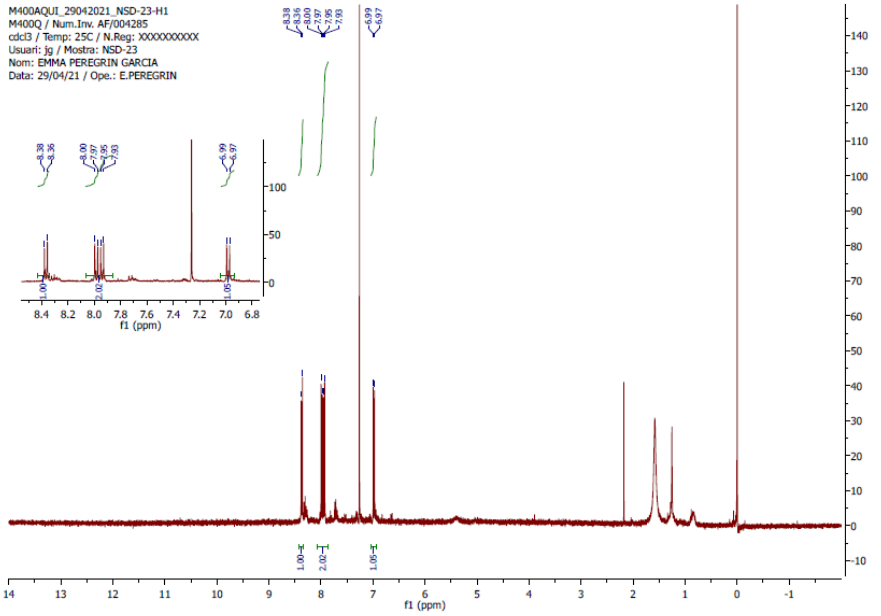

Fig 5 ^{1}H-NMR compound **3**

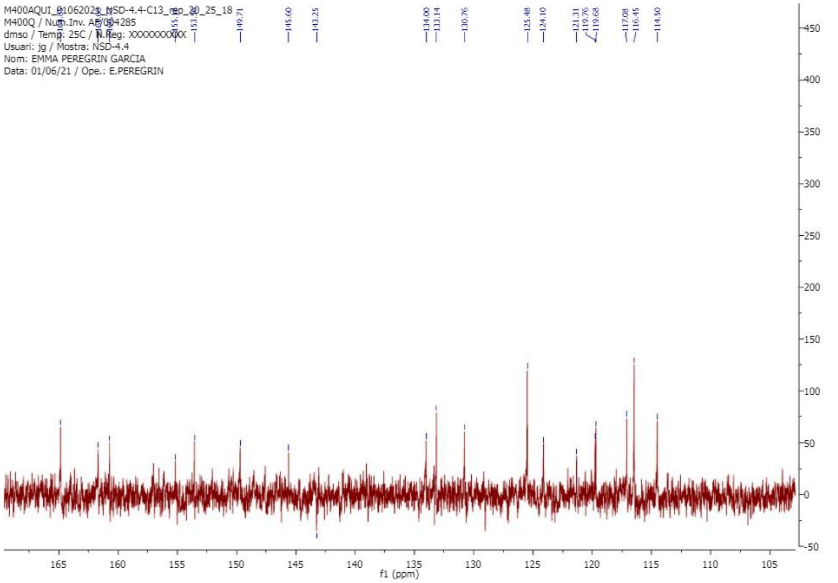

Fig 6 ^{13}C-NMR compound **3**

COMPOUND 4

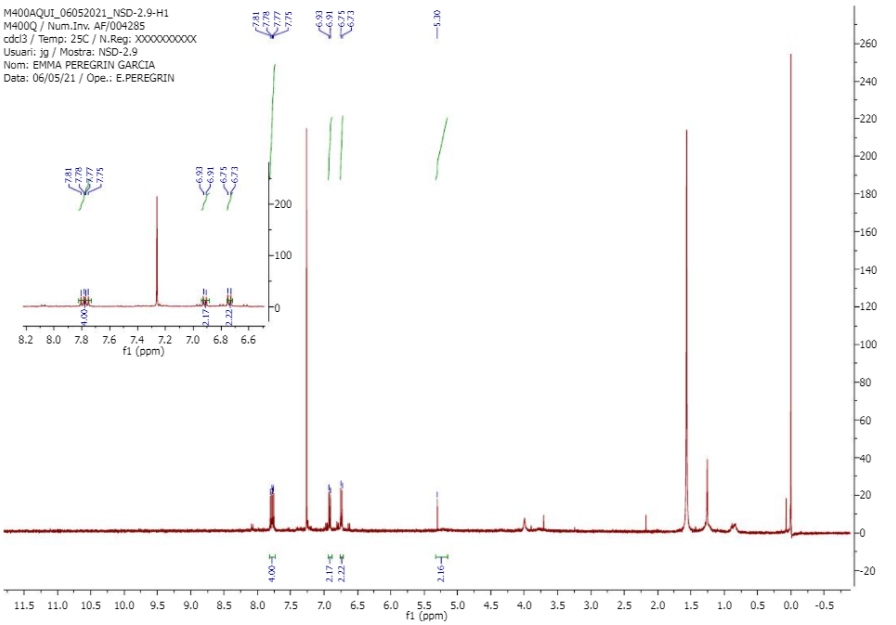

Fig 7 ^{1}H-NMR compound **4**

COMPOUD 5

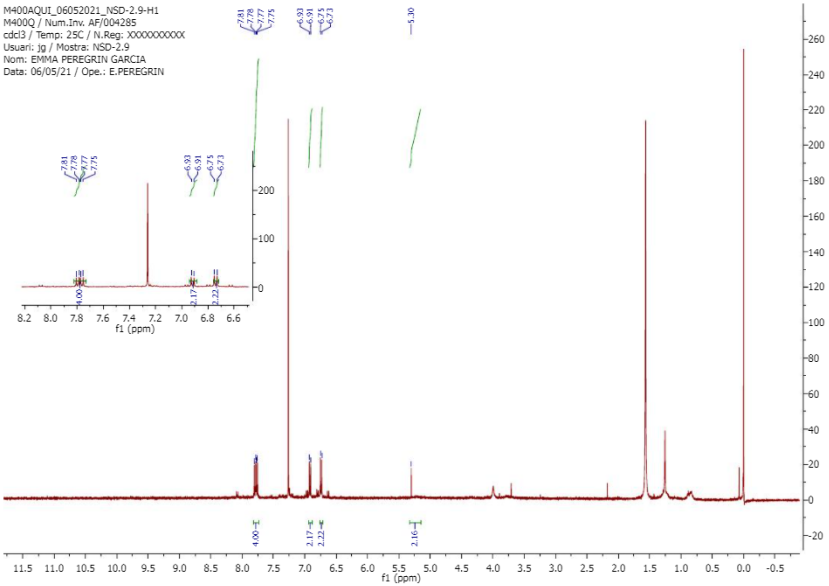

Fig 8 ^{1}H-NMR compound **5**

COMPOUND 6

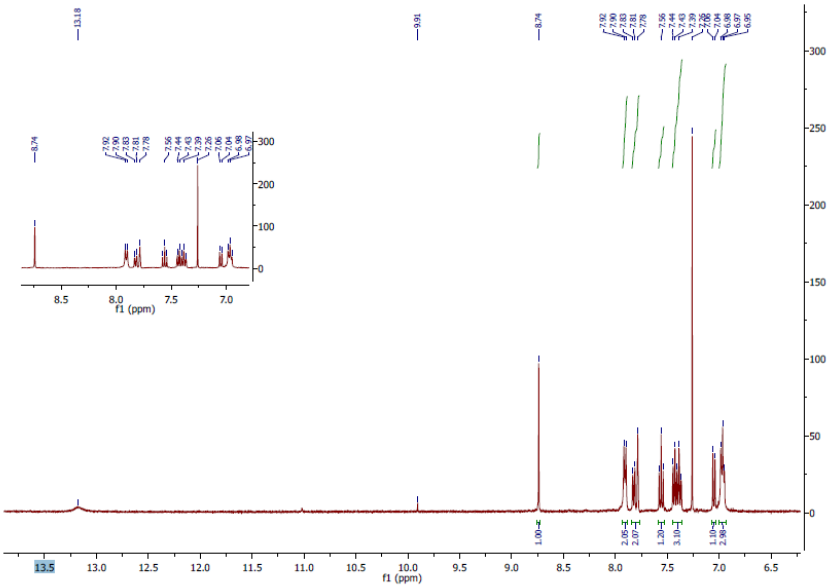

Fig 9 ^{1}H-NMR compound **6**

COMPOUND 7

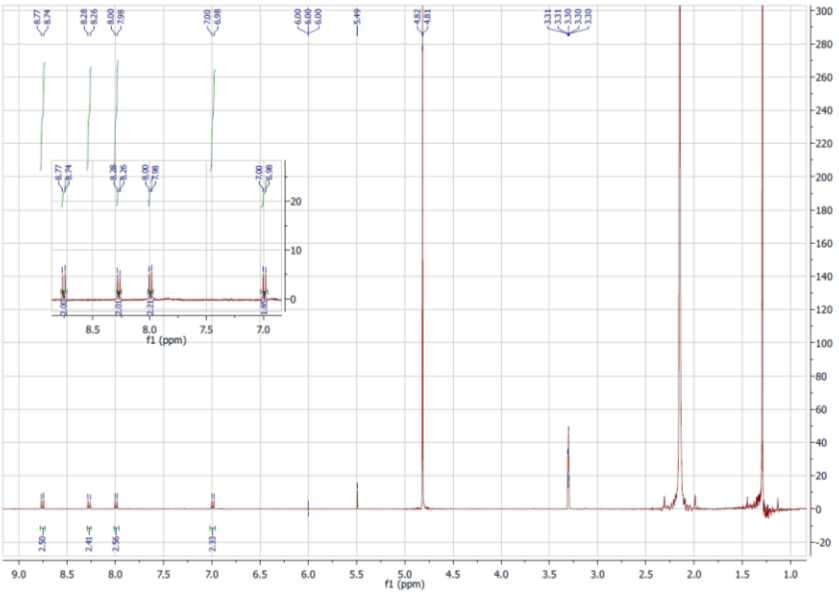

Fig 10 ^{1}H-NMR compound **7**